

STRUCTURE OF THE MAGNETIC FIELD IN THE RADIO JETS IN 3C 31 AND NGC 315

E. B. FOMALONT

National Radio Astronomy Observatory, Green Bank, West Virginia¹

A. H. BRIDLE

Queen's University at Kingston, Ontario

A. G. WILLIS

Netherlands Foundation for Radio Astronomy, Radiosterrenwacht Westerbork, The Netherlands

AND

R. A. PERLEY

National Radio Astronomy Observatory, Socorro, New Mexico¹

Received 1979 August 16; accepted 1979 October 9

ABSTRACT

We have used the VLA to map the distributions of the total and linearly polarized radio brightness over the inner parts of the jets in the radio galaxies 3C 31 and NGC 315. In each galaxy we find that the jet on one side of the nuclear radio core has a bright base within which the organized component of the magnetic field lies predominantly parallel to the jet for several kiloparsecs. Farther from the cores, as the jets widen, their magnetic fields become predominantly perpendicular to the jet axes, and the jets become more symmetric in intensity.

These changes in magnetic-field direction are consistent with some classes of continuous-beam models for energy transport in extragalactic radio sources. The details of the polarization distributions can be fitted to a model wherein the ordered magnetic-field components in the beams have helical configurations whose pitch angles increase with distance from the radio cores.

Subject headings: galaxies: individual — magnetic fields — polarization —
 radio sources: galaxies

I. INTRODUCTION

Several radio galaxies are now known in which bright, highly-collimated, and continuous jets of radio emission link a small-diameter central source (radio core) to the diffuse outer lobes. Examples are NGC 315 (Bridle *et al.* 1976, 1979), 3C 31 (Burch 1977, 1979), NGC 6251 (Waggett, Warner, and Baldwin 1977), and 3C 449 (Perley, Willis, and Scott 1979). These radio jets probably arise from inefficiencies in the mechanism by which fresh relativistic particles are transported outward from radio-galaxy nuclei to replenish the energy reservoirs in their outer lobes. In many radio galaxies the transport mechanism may be highly efficient and thus unobservable. Studies of the radio galaxies which have dissipative, radio-luminous jets may, however, provide some insights into physical processes that could occur within the "energy pipelines" of all extended extragalactic sources. For this reason, we have begun a series of high-resolution studies of radio jets using the Very Large Array (VLA) now under construction by NRAO in New Mexico.

This paper presents new high-resolution maps of the distributions of linear polarization over the inner parts of the jets in the radio galaxies 3C 31 and NGC 315. We find that the jets in both of these sources contain similar well-organized polarization distribu-

tions which imply that their magnetic field structures evolve with distance from the radio core as expected if the jets are emission from within expanding beams containing both relativistic particles and magnetic fields.

II. THE VLA OBSERVATIONS OF 3C 31

The source 3C 31 (0104+321 = NGC 383) was observed with 13 antennas of the partially completed VLA at 1.480 and 4.885 GHz (20 cm and 6 cm) in 1978 November and December. Table 1 lists the main parameters of the observations. Because most of the antennas were located on the west arm of the VLA there were gaps in the coverage of the (u, v) plane, and the CLEAN deconvolution algorithm (Högbom 1974) was used to reduce the effects of the $\sim 10\%$ sidelobes resulting from these gaps. The shortest antenna spacings were 226 m at 20 cm and 486 m at 6 cm; structural scales $\gtrsim 90''$ at 20 cm and $\gtrsim 12''$ at 6 cm in their narrowest dimension are therefore attenuated in the derived maps. Observations at 6 cm of the inner $30''$ of the radio jets should not be significantly affected by the missing information, but we caution readers against using the maps below to derive detailed spectral index variations across the source.

Figure 1 shows the 20 cm map of the inner $\sim 350''$ (170 kpc with $H_0 = 50 \text{ km s}^{-1} \text{ Mpc}^{-1}$) of 3C 31 with a resolution (FWHM) of $2''.5$ by $5''.0$ (major axis in p.a. 150°). The main features of this map are very

¹ Operated by Associated Universities, Inc., under contract with the National Science Foundation.

MAGNETIC STRUCTURE OF RADIO JETS

419

TABLE 1
PARAMETERS OF VLA OBSERVATIONS OF 3C 31

System temperature.....	50 K	
Bandwidth.....	50 MHz	
Calibration source.....	0116+319:	$\alpha = 01^{\text{h}}16^{\text{m}}47^{\text{s}}.245,$ $\delta = 31^{\circ}55'05''.78$
Source scan length.....	12 minutes	
Calibrator scan length.....	3 minutes	
	1480 MHz	4885 MHz
Observing date(s).....	1978 Nov 28/Dec 2	1978 Dec 16
Hour angle range.....	$-7^{\text{h}}1$ to $+6^{\text{h}}6$	$-4^{\text{h}}4$ to $+6^{\text{h}}6$
Primary beamwidth (FWHM).....	32'	9'
Polarizations observed.....	Orthogonal linear	Opposite circular
Flux density of calibrator.....	2.62 Jy	1.57 Jy

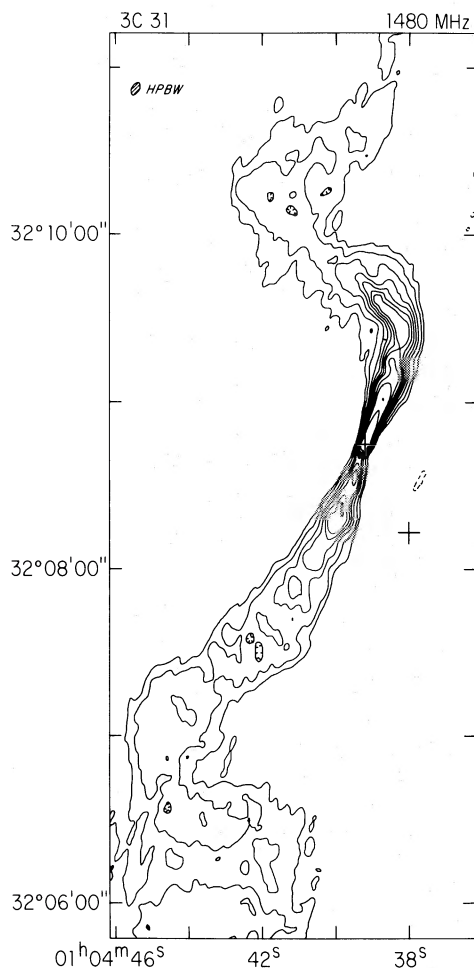
*Antenna positions (meters):*East arm (azimuth $114^{\circ}59'42''$) -80.00, 484.00, 970.50, 1589.92West arm (azimuth $236^{\circ}00'03''$) 484.00, 709.79,^a 970.50,^b 1589.92,^c 3188.09, 5222.90,^c 7659.48, 10472.87, 13643.92,^c 17157.23^b^a Used only at 1480 MHz.^b Used only at 4885 MHz.^c Only one polarization available at 4885 MHz.

FIG. 1.—Contour map of 3C 31 at 20 cm. The contour levels are -1.5 (dashed), 1.5, 3, 6, 9, 12, 15, 18, 24, 30, 45 mJy per beam. The full-width half power beam is shown in the upper left. The nuclei of the galaxies NGC 383, coincident with the radio core, and NGC 382 are shown by the crosses.

similar to those of the 11 cm maps at $3''.7$ by $7''.0$ resolution shown by Burch (1977, 1979). Both jets widen with an opening angle of $\sim 15^{\circ}$ from the radio core and eventually deflect eastward before merging into the more complex diffuse lobes. The deflections have been interpreted by Blandford and Icke (1978) as the result of a gravitational interaction between NGC 383 and its neighbor NGC 382. The positions of these galaxies are marked by crosses in Figure 1.

Figure 2a shows a 6 cm map at the same resolution as Figure 1. Except near the radio core, the 6 cm emission is weaker because of the $\nu^{-0.5}$ spectrum of the radiation. Superposed on the contour map are vectors which indicate the distribution of the linearly-polarized emission; their lengths are proportional to the polarized intensity at each point, and their directions show the position angles of the E vectors. The E vectors generally lie along the axis of extension of the jets except in a region just north of the radio core and along the extreme edges of the jets. Figure 2b shows a 6 cm map of the lower $25''$ (12 kpc) of the northern jet at a resolution of $0''.55$ by $1''.49$ (major axis in p.a. 151°). The widening of the jet as it leaves the radio core, and its generally smooth structure, are clear on this map, which also shows the distribution of the linearly polarized emission at $0''.55$ by $1''.49$ resolution.

The weaker southern jet is close to the noise in the map at this resolution; even the most intense regions near the base of the southern jet on the 20 cm map (Fig. 1) contain no 6 cm emission brighter than 1.6 mJy per beam at this resolution. This lack of fine structure in the southern jet contrasts with the elongated feature (peak intensity 9.8 mJy per beam) at the base of the northern jet.

Recently Butcher, van Breugel, and Miley (1980) using a TV camera at the Kitt Peak 4 m telescope have found an optical jet emanating to the north from the center of NGC 383, the parent optical galaxy of 3C 31. This optical jet coincides with, and has approximately the same size and orientation as, the elongated

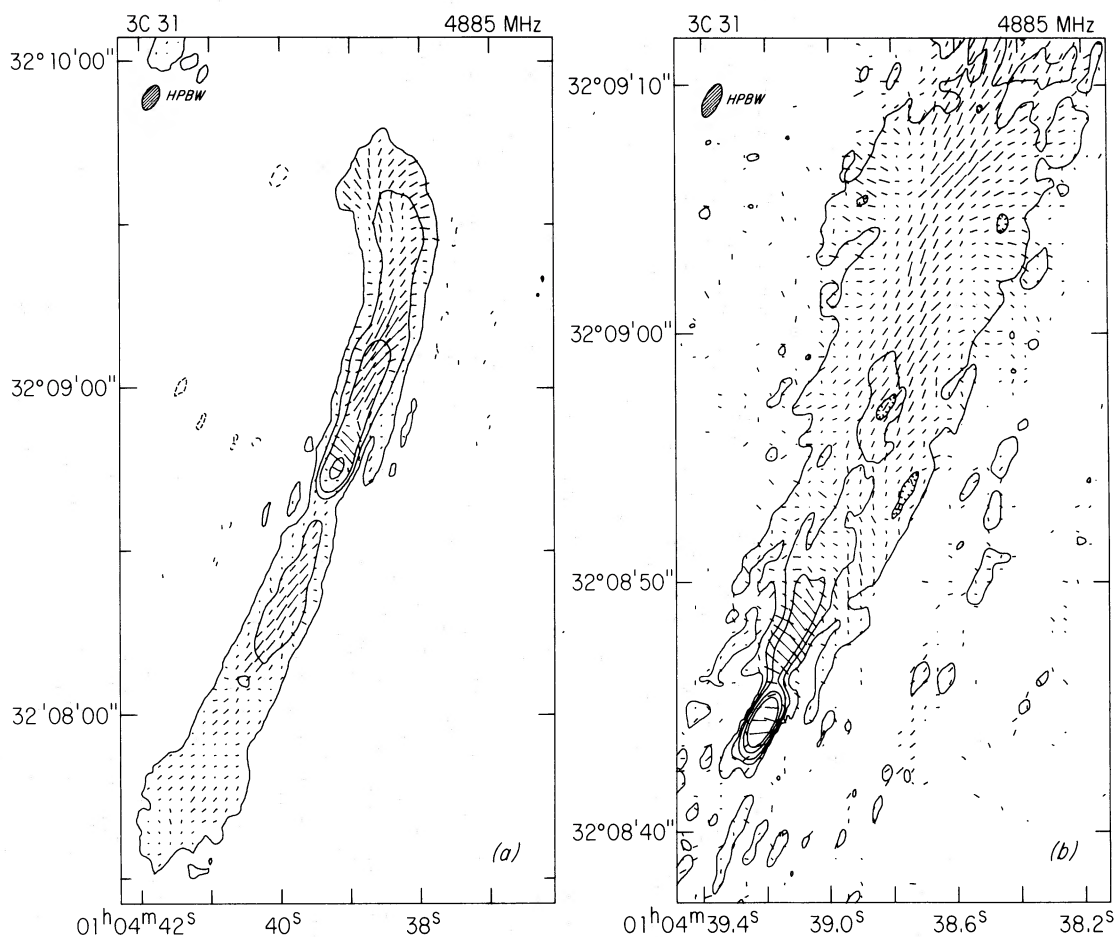


FIG. 2.—Contour maps of 3C 31 at 6 cm. The total intensity is shown by the contours. The linear polarization is indicated by the line segments whose lengths are proportional to the intensities and whose angles equal the E vector orientations: (a) resolution of 5.0×2.5 . Contour levels are -1 (dashed), 1, 4, 10, 50 mJy per beam (the longest polarized intensity vector corresponds to 5.2 mJy per beam); and (b) resolution of 1.49×0.58 . Contour levels are 0.8, 2.4, 4.8, 12, 24 mJy per beam. The longest polarized intensity vector corresponds to 1.8 mJy per beam.

radio feature at the base of the northern radio jet. Also, just as the radio observations show that there are no very compact features to the south of the nucleus in the southern jet, so there apparently is no optical jet extending to the south.

III. THE POLARIZATION STRUCTURE OF THE JETS IN 3C 31

Figure 3a shows the 6 cm peak intensity I along the inner $25''$ of the northern jet as a function of the angular distance θ from the radio core, obtained from the map in Figure 2b. The resolution is $1.4''$ along the jet. Figures 3b and 3c show the variations of the degree of linear polarization, $p = (Q^2 + U^2)^{1/2}/I$ and of the position angle of the E vector, χ , with θ . Estimated errors are shown for a few representative points.

Within $\theta \lesssim 1.5''$ of the radio core, its emission dominates that of the jet. The core is only slightly polarized, with $p = 1 \pm 0.5\%$. For $\theta > 1.5''$, I and p both increase, reaching maxima near $\theta \approx 4''$ (2 kpc) from the core. Throughout this regime, which we will

call the “base” of the jet, χ varies between 60° and 40° . The maximum value of p is $\sim 18\%$.

For $4'' \lesssim \theta \lesssim 9''$ the degree of polarization falls steadily to a value near zero. Thereafter a new polarization angle near 150° is established and a highly-organized polarization with the E vectors within $\pm 10^\circ$ of this value is maintained beyond $\theta \sim 12''$. This highly-organized polarization is roughly perpendicular to that just before the polarization minimum at $\theta = 9''$. We will call the regime $4'' < \theta \leq 12''$ (2–6 kpc) the “transition” regime, and the regime beyond $\theta = 12''$ the “well-ordered” regime in what follows.

Figures 4a, b, and c plot the parameters I , p and χ as functions of θ from the lower-resolution 6 cm map in Figure 2a; at this resolution ($4''$ along the jet) there is a sufficiently large signal-to-noise ratio to show the polarization properties of both jets until they deflect eastward before entering the lobes. The degree of polarization p shows large oscillations about a typical value of $\sim 25\%$ in the well-ordered regime. The oscillations appear to have a wavelength of about

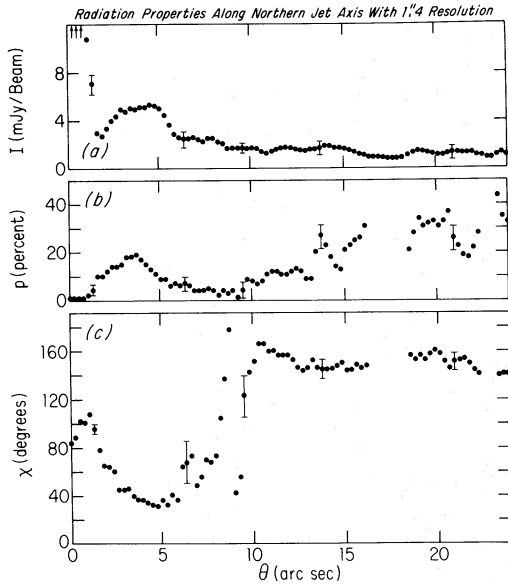


FIG. 3.—(a) surface intensity I , (b) degree of linear polarization p , and (c) orientation of E vector χ along the axis of the northern jet in 3C 31 as a function of θ angular distance from the radio core. Selected error bars of 2σ are shown. The distributions were made from Fig. 2b with a resolution of $1.4''$ along the jet.

$12''$ (5.7 kpc) in Figure 4b. Smaller oscillations with a wavelength of about $3''$ (1.4 kpc) are also apparent in Figure 3b; these shorter wavelength oscillations, if they persist down the jet, would be averaged out in the lower resolution display of Figure 4. I and χ show

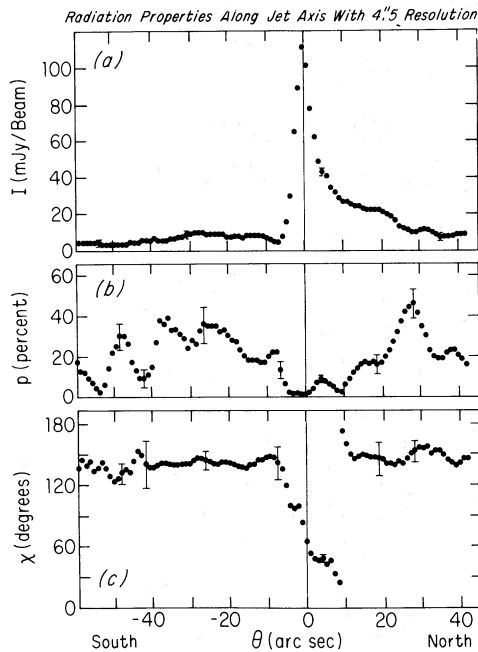


FIG. 4.—(a) surface intensity I , (b) degree of linear polarization p , and (c) orientation of E vector χ along the axes of both jets in 3C 31 as a function of θ angular distance from the radio core. Selected error bars of 2σ are shown. The distributions were made from Fig. 2a with a resolution of $4''$ along the jet.

little sign of variations that correlate with the oscillations in p .

Some fine structure is seen in the polarization across the jets. At the base of the jet and in the transition regime before the polarization minimum at $\theta = 9''$, p in the northern jet has maxima at the edges of the jet and a minimum at its center. In the well-ordered regimes of both jets p has a maximum near the center and minima at the edges; the variations of p along the centers of the jets are also seen toward their edges. The position angles of the E vectors near the edges of the jets in the well-ordered regime are perpendicular to those at the centers of the jets.

IV. THE POLARIZATION STRUCTURE OF THE JET IN NGC 315

Similar polarization structure exists in the inner $60''$ of the main (northwestern) jet of NGC 315 at 6 cm. Figure 5 shows a map of total and polarized intensities at $3.4''$ by $6.7''$ resolution (major axis in p.a. 177°) over the inner $90''$ (43 kpc) of this jet, obtained by tapering the 6 cm data of Bridle *et al.* (1979) with a Gaussian function falling to 50% at 4.0 km from the array center. We again find (a) an initial increase in p from near zero at the radio core to 14% shortly before the peak intensity, which occurs at $\theta = 5''$ (2.4 kpc), (b) a decline in p beginning shortly before $\theta = 5''$ and continuing to $p \approx 0\%$ at $\theta \approx 24''$ (11 kpc) and (c) the subsequent appearance of a well-ordered polarization with p oscillating between $\sim 10\%$ and $\sim 20\%$ in a position angle approximately perpendicular to that observed just before the polarization minimum. Because of the relatively poor signal-to-noise ratio, further details of the polarization distribution are not discernable. A regime of extremely high ($p \approx 60$ to 70%) polarization and well-ordered E vectors also

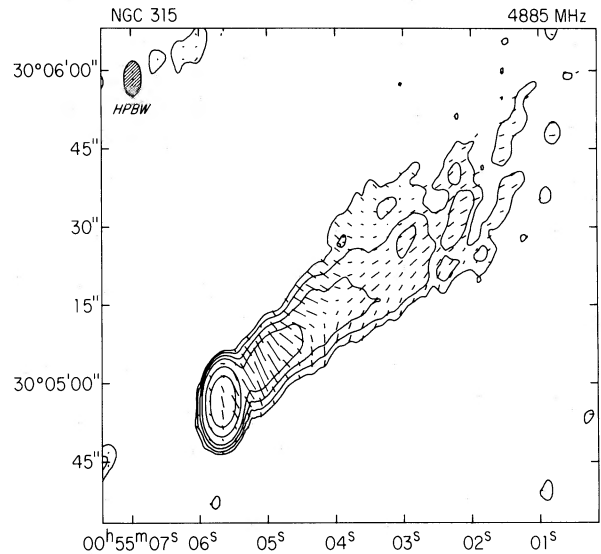


FIG. 5.—Contour map of NGC 315 at 6 cm. The contour levels for the total intensity are 1, 2, 4, 8, 30, 100 mJy per beam. The linear polarization is indicated by the line segments. The longest line corresponds to 1.8 mJy per beam. The full-width half power beam is shown in the upper left.

exists in the outer parts of this jet (Bridle *et al.* 1979; Willis *et al.* 1980).

We can therefore again distinguish a base regime, where for the first ~ 2 kpc of the jet both I and p increase, followed by a transition regime, in this case extending to $\theta \approx 28''$ (13 kpc), in which the initial polarization disappears and is replaced by a new polarization approximately at right angles to it. As in 3C 31, p increases, with some oscillations, throughout the following well-ordered regime, while χ remains essentially constant.

V. MAGNETIC FIELD CONFIGURATIONS IN 3C 31 AND NGC 315

We have combined our 6 cm polarization data with those of Burch (1979) at 11 cm to find the orientation of the projected magnetic field in the 3C 31 jets. Assuming that no ambiguity of position-angle rotation arises between 11 cm and 6 cm we find an average rotation measure $RM = -62 \text{ rad m}^{-2}$ in both jets, in good agreement with the value $RM = -63 \pm 5 \text{ rad m}^{-2}$ derived from the integrated polarization over a wider wavelength range by Burch (1979). The intrinsic (zero wavelength) E vectors would be rotated 13° counterclockwise from our 6 cm vectors if this RM applies throughout the structure. (This assumption may fail at the base of the jets where particle densities and field strengths are likely to be greatest, and Burch's data are not of sufficient resolution to verify the value of RM directly.)

On the axis of the northern jet in 3C 31, the magnetic field, assumed perpendicular to the zero wavelength E vectors, therefore lies predominantly *perpendicular* to the length of the jet in the well-ordered regime. At the edge of the jet in this regime, the field is predominantly parallel to the jet. If RM near the base of the jet is close to the average value of -62 rad m^{-2} , the field must be predominantly *parallel* to the length of the jet at its base. The lower resolution data in Figure 2(a) show that the southern jet has the same field structure in its well-ordered regime, but lacks the base regime in polarization, just as it lacks this regime in total intensity.

For NGC 315, polarization maps from the Westerbork telescope at 50 cm and 21 cm (Willis *et al.* 1980) have been combined with the 11 cm data of Stoffel and Wielebinski (1978) to give $RM = -82 \text{ rad m}^{-2}$ over the region mapped in Figure 5. If this RM applies over all of Figure 5, the magnetic field would be predominantly parallel to the length of the jet in the base and nearer transition regimes, and predominantly perpendicular to it throughout the well-ordered regime.

The values we have derived for RM for both 3C 31 and NGC 315 are similar to those of other sources in the same area of sky (Simard-Normandin and Kronberg 1979), so the observed rotation is probably mainly due to foreground material in the interstellar medium of our galaxy.

VI. DISCUSSION

The magnetic field configurations in both of these dissipative jets evolve with distance from their

galactic nuclei much as expected from continuous-beam models of extragalactic sources (Blandford and Rees 1974, 1978) if (a) we are detecting radiation from the body of the beam itself rather than from a lossy sheath surrounding it, and (b) the fields are frozen into an expanding flow of thermal plasma accompanying the beam of relativistic particles.

The dominance of B_{\parallel} in the base regimes of both 3C 31 and NGC 315 is understandable if the fields in the first few kpc of these jets have been frozen into collimated flows which initially stretched them predominantly in the direction away from the radio cores. As such beams later expand more freely, the B_{\parallel} component should decrease faster than the B_{\perp} component (Blandford and Rees 1978). In the transition regime of these two sources, B_{\perp} becomes comparable to B_{\parallel} , and in the well-ordered regime B_{\perp} has become dominant. The fact that we observe such a transition is evidence that the jet emission comes from the beam itself rather than from a lossy sheath around it (in which the field would be stretched parallel to the length of the jet at all distances from the radio core). Since the change of dominance from B_{\parallel} to B_{\perp} occurs over a distance in which the jet widths expand by only a factor of 3 to 5, B_{\parallel} in the organized field cannot exceed B_{\perp} by more than a factor ~ 3 near the bases of the jets.

The magnetic field structure, whose projection we see as B_{\perp} , is probably a circumferential field configuration, to satisfy $\nabla \cdot \mathbf{B} = 0$ (the B_{\parallel} components may satisfy this condition by returning to the galaxy outside the synchrotron-emitting volume). Near the base of the jet where B_{\parallel} dominates, the total organized magnetic field must resemble a helix of pitch angle $\sim 20^\circ$ with respect to the jet axis, while in the well-ordered regime the pitch angle of the helix must be $\gtrsim 70^\circ$.

Several details of the polarization characteristics of 3C 31 are consistent with such a helical field configuration: (a) in a helix of pitch angle $\sim 20^\circ$ the field component perpendicular to the line of sight would appear most organized at the edges of the beam, accounting for the observed minima of p on the jet axis in the base regime; (b) where the pitch angle is $\sim 45^\circ$, the polarization of the emission received from opposite sides of the beam would nearly cancel, accounting for the low values of p observed in the transition regime; and (c) in a helix of pitch angle $\gtrsim 70^\circ$ the most organized field components perpendicular to the line of sight would be found on the jet axis, accounting for the observed maxima of p on the axis in the well-ordered regime. The weaker perpendicular polarization at the edges of both 3C 31 jets in the well-ordered regime is also consistent with the helical field geometry. This polarization "flip" across the jets should be most striking if they point at a small angle to the line of sight, so that the helical field is seen in a nearly circular cross section. The parallel field at the edges of the 3C 31 jets might also result from field shearing at the boundaries of the beams, but we note that Blandford and Icke (1978) required the jets to be at only 10° to the line of sight in order to fit their structure to a dynamical model of the NGC 382/383 system.

The one-sided appearance of the bright fine structure in the base regimes of 3C 31 and NGC 315 and other "jet" radio sources could be caused by a relativistic intensity asymmetry between the blueshifted and redshifted sides of the flow. Such an effect need only require a bulk velocity in the line of sight of $\sim 0.3c$.

The initial increases of the brightness of the jets at their bases could be due to (a) increasing numbers of relativistic particles, (b) magnetic field amplification in the flow, or (c) increasing randomization of the pitch angles of the relativistic particles with respect to the field components that are perpendicular to the line of sight. Beyond the base regime these effects must be offset by the reduction of the synchrotron emissivity due to expansion of the particle and magnetic fluxes, so that the peak intensity of the jets decreases throughout this regime. In fact, the surface brightness of the jets actually decreases far more slowly than would be expected on the basis of simple expanding fluxes of particles and fields. If the strength of the magnetic field in the jets is proportional to r^{-1} as the jets expand, then the surface brightness of the jets would be expected to be proportional to $r^{-(2+7\alpha/3)}$ (e.g., Burch 1979), which for 3C 31 is $\sim r^{-3}$. Over the angular distance between 5" and 20" from the nucleus of 3C 31, the width of the jet (FWHM) increases from 1" to 6". Consequently, the surface brightness would have decreased by a factor of 6^3 (216), and the jet would have ceased to be visible. However, the actual drop in brightness over this angular distance is only about a factor of 4. Thus, in the expanding beam models an additional source of energy must be invoked in the outer parts of radio jets to amplify the magnetic field and/or produce a larger population of relativistic particles. This source of energy might be the bulk kinetic energy of nonrelativistic thermal plasma in the jet (see Blandford and Icke 1978; Perley, Willis, and Scott 1979).

The large variations in the degree of polarization in the well-ordered regimes of the jets in 3C 31 may be associated with instabilities in the flow along these jets; the circumferential component of the magnetic

field may become more disordered near unstable regions of the flow with resulting depolarization across the jet in these regions. Figure 1 shows that the position angle of the northern jet also oscillates on a scale similar to that of the longer wavelength oscillations in p , shortly before the sharp eastward deflection. This behavior is reminiscent of the classical "kink" instability in plasma columns with dynamically significant circumferential magnetic fields enclosing axial currents and field components, although a similar instability may be produced by purely hydrodynamic boundary oscillations (Hardee 1979).

The polarization structure of the jets in 3C 449 has been observed by Perley, Willis, and Scott (1979) at distances from its radio core which correspond to the well-ordered regimes in 3C 31 and NGC 315. The dominant magnetic field component in these jets also lies perpendicular to their length, although the rotation measure in 3C 449 is less certain than it is for 3C 31 and NGC 315. The field structures we have found in 3C 31 and NGC 315 may therefore be typical of other jets in radio galaxies of relatively low radio luminosity. Clearly at $\sim 1''$ resolution, the VLA is resolving these relatively nearby jets into regimes with well-organized polarizations which imply that physical magnetic field configurations are not being seriously smeared by the synthesized beam. Studies of such jets with the same high resolution at 20 cm, 6 cm, and 2 cm using the finished VLA should therefore provide maps of physically meaningful spectral, Faraday-rotation and depolarization parameters for comparison with detailed models of relativistic beam dynamics.

We thank the VLA staff for their support of these observations, and J. J. Palimaka for assistance with the data reduction. This work was partially supported by grants to A. H. B. from the Natural Sciences and Engineering Research Council of Canada, and to A. G. W. from the National Science Foundation while at Brandeis University.

REFERENCES

- Blandford, R. D., and Icke, V. 1978, *M.N.R.A.S.*, **185**, 527.
 Blandford, R. D., and Rees, M. J. 1974, *M.N.R.A.S.*, **169**, 395.
 ———. 1978, *Phys. Scripta*, **17**, 265.
 Bridle, A. H., Davis, M. M., Fomalont, E. B., Willis, A. G., and Strom, R. G. 1979, *Ap. J. (Letters)*, **228**, L9.
 Bridle, A. H., Davis, M. M., Meloy, D. A., Fomalont, E. B., Willis, A. G., and Strom, R. G. 1976, *Nature*, **262**, 179.
 Burch, S. F. 1977, *M.N.R.A.S.*, **181**, 599.
 ———. 1979, *M.N.R.A.S.*, **187**, 187.
 Butcher, H., van Breugel, W., and Miley, G. K. 1980, *Ap. J.*, **235**, 749.
 Hardee, P. E. 1979, *Ap. J.*, in press.
 Högbom, J. A. 1974, *Astr. Ap. Suppl.*, **15**, 417.
 Perley, R. A., Willis, A. G., and Scott, J. S. 1979, *Nature*, **281**, 437.
 Simard-Normandin, M., and Kronberg, P. P. 1979, *Nature*, **279**, 115.
 Stoffel, H., and Wielebinski, R. 1978, *Astr. Ap.*, **68**, 307.
 Waggett, P. C., Warner, P. J., and Baldwin, J. E. 1977, *M.N.R.A.S.*, **181**, 465.
 Willis, A. G., Strom, R. G., Bridle, A. H., and Fomalont, E. B. 1980, in preparation.

A. H. BRIDLE: Department of Physics, Stirling Hall, Queen's University at Kingston, Ontario K7L 3N6, Canada

E. B. FOMALONT: National Radio Astronomy Observatory, Edgemont Road, Charlottesville, VA 22901

R. A. PERLEY: National Radio Astronomy Observatory, P.O. Box "O", Socorro, NM 87801

A. G. WILLIS: Netherlands Foundation for Radio Astronomy, Radiosterrenwacht Westerbork, Schattenberg 4, 9433 TA Zwiggelte, The Netherlands